AN ABSTRACT OF THE THESIS OF

Robert E Hawkins for the degree of Master of Science in Physics presented on July 25, 2002.

Title: ^{13}C–CP MAS NMR Study of Decomposition of Five Coniferous Woody Roots From Oregon.

Abstract approved Redacted for privacy
William W. Warren

Using ^{13}C cross polarization magic angle spinning nuclear magnetic resonance techniques on 5 species of dead trees from the northwest (western hemlock, Douglas fir, Sitka spruce, lodgepole pine and ponderosa pine) I tracked the lignin and cellulose content over a 22 to 36 year period in order to determine the effects of decay fungi, if any, that is attacking certain species of tree. I had samples from the wood of the roots, the bark on the roots and, in some cases, the resin core of the roots. The Department of Forest Science at Oregon State University has studied this problem by using wet chemical analysis, and direct visual observation. Mark Harmon and Hua Chen of the Department of Forest Science believe that white rot occurred most frequently in the lodgepole pine and ponderosa pine and brown rot was more frequent in the Douglas-fir and Sitka spruce. Western hemlock seemed to have both brown and white rots active.

The Douglas fir bark sample showed definite decomposition consistent with white rot during the first 10 years. The ponderosa pine sap showed decomposition consistent with white rot in the 10 to 22 year period. Sitka Spruce showed some decomposition consistent with white rot in the bark from 7 to 33 years, and the western hemlock showed some decomposition consistent with white rot in the sap in the first 10 years.

The decompositions consistent with brown rot were much easier to see in this study. Virtually all the sap and bark samples showed decomposition consistent with brown rot at some point. The Douglas fir was the only species, other than lodgepole pine, not to show any decomposition consistent with brown rot in the bark of the tree, only decomposition

consistent with white rot. The Douglas fir did show a decay consistent with brown rot in the sap for the first ten years. Ponderosa pine showed evidence of decay that brown rot would cause for the first 10 years in the sap and the bark. The Sitka spruce species analysis showed brown rot type decay in the bark for the first 7 years and in the sap for the entire time studied of 33 years. The lodgepole pine was the only species to not show any brown rot type decay in the sap or bark for the entire 22 year period studied. The western hemlock was distinct by not showing any definitive brown rot type decay for the first 10 years, but showed massive decay consistent with brown rot in both sap and bark during the following 26 years studied.

I used an 8 Tesla magnet and the MAS frequency was at 5 kHz. The recycle time was 1.5 seconds and the contact time was 1 ms. I generally took about 10,000 acquisitions per sample, which added up to about 4 hours total acquisition time per sample.

Presence of these rots shows that certain species are more susceptible than others, and also shows that local environmental conditions can contribute to rot susceptibility.

^{13}C–CP MAS NMR Study of Decomposition of Five Coniferous Woody Roots From Oregon.

by

Robert E Hawkins

A THESIS

Submitted to

Oregon State University

in partial fulfillment of
the requirements of the
degree of

Master of Science

Presented July 25, 2002
Commencement June 2003

Master of Science thesis of Robert E Hawkins presented on July 25, 2002.

APPROVED:

Redacted for privacy

Major Professor, representing Physics

Redacted for privacy

Head of the Department of Physics

Redacted for privacy

Dean of the Graduate School

I understand that my thesis will become part of the permanent collection of Oregon State University libraries. My signature below authorizes release of my thesis to any reader upon request.

Redacted for privacy

Robert E Hawkins, Author

ACKNOWLEDGMENTS

I would like to express sincere appreciation to Professor William W. Warren for his help, guidance, funding, and all the time he spent helping me with my research and thesis. I would also like to thank Hua Chen and Mark Harmon of the Oregon State University Department of Forest Science for their time, knowledge, funding, and for the samples prepared and supplied.

TABLE OF CONTENTS

TABLE OF CONTENTS (CONTINUED)

LIST OF FIGURES

LIST OF TABLES

^{13}C–CP MAS NMR Study of Decomposition of Five Coniferous Woody Roots From Oregon

1. INTRODUCTION

1.1 BACKGROUND

Knowledge of decomposition in different species of tree in the northwest, and the rate of decomposition in these species is of great interest, and can be readily put to important use. There is of course the academic interest of understanding lignin decomposition but there are practical applications as well. White rot acts to decompose both lignin and the cellulose, which makes up most of the wood. Both white and brown rot, like most living organisms, thrive in certain climates. The locations of these trees and the weather they experience is therefore vital to having a complete understanding of the decomposition mechanism.

If white rot attacks a tree, over time it will create hollow channels in the soil as the roots decompose. Brown rot does not decompose the roots nearly as much because it only attacks the cellulose, so in turn does not create hollow channels to nearly the degree that white rot does. Hollow channels created by white rot can have a dramatic effect on soil stability if new roots have not had a chance to form and strengthen the soil. Understanding the rate of decomposition of these roots will aid in predicting when and where soil erosion and landslides could potentially occur. Hollow channels are also important in regulating soil water movement and providing habitats for soil animals (Chen H. et al., 2001).

1.2 FOCUS OF THIS STUDY

The focus of this study was to track the lignin and cellulose content as a function of time in order to determine the kind of rot, if any, that is attacking certain species of tree. Lignin and cellulose are two different organic compounds (shown in Fig. 6) that, together, make up most of a tree's mass. The species of trees studied were lodgepole pine from Pringle

Falls, ponderosa pine from Pringle Falls, Sitka spruce from Cascade Head, western hemlock from Cascade Head, and Douglas fir from H.J. Andrews (See Map, Fig. 1). Depending on what kind(s) of rot are acting on the tree (white and/or brown), the ratio of lignin to cellulose content can change over time.

Brown rot in trees only attacks the cellulose part of the tree (Preston, C.M. et al., Forest Ecology and Management, 1998). When brown rot attacks a tree, what's left behind mostly consists of lignin. Therefore the ratio of lignin to the rest of the mass of the tree will increase. White rot is believed to attack both the cellulose and lignin molecules (Preston C.M., 1998), so over time the total mass will decline but the ratio of lignin to cellulose may stay relatively unchanged.

In order to determine the change in lignin and cellulose, two, or when possible three, different ages were looked at for each species of tree. For each time period, one or two samples were taken from two or three different parts of the tree; the sap wood, the bark, and when possible, the resin core. In all, for the five species studied, there were 69 different samples (see table 1).

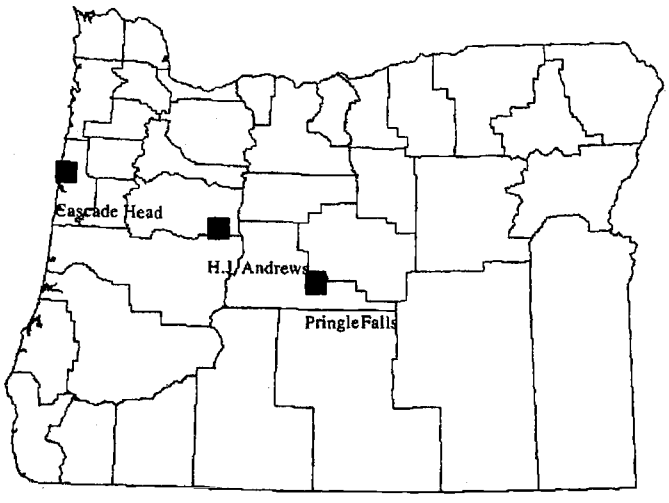

Figure 1. Map of Oregon indicating location where samples were taken (Chen H).

	lodgepole pine	ponderosa pine	Douglas fir	Sitka spruce	western hemlock
Sap Wood	2-Fresh	2-1 Yr old	2-Fresh	2-Fresh	2-Fresh
	2-10 Yr old	2-10 Yr old	2-10 Yr old	2-7 Yr old	2-10 Yr old
	2-22 Yr old	2-22 Yr old	1-36 Yr old	2-33 Yr old	2-36 Yr old
Bark	2-Fresh	2-1 Yr old	2-Fresh	2-Fresh	2-Fresh
	2-10 Yr old	2-10 Yr old	2-10 Yr old	2-7 Yr old	2-10 Yr old
	2-22 Yr old	2-22 Yr old	1-36 Yr old	1-33 Yr old	2-36 Yr old
Resin Core	X	X	X	2-Fresh	X
	X	X	2-10 Yr old	2-7 Yr old	X
	2-22 Yr old	X	2-36 Yr old	2-33 Yr old	X

Table 1. Table showing number and age of samples. Each column lists the species and three major rows for part of tree sample was taken from.

1.3 GOALS OF THIS STUDY

The goal or purpose of this study was to carry out an independent measurement of lignin and cellulose ratios that can be compared with previous results obtained by using wet chemical analysis, and direct visual observation. Mark Harmon and Hua Chen from the Department of Forest Science believe that white rot occurred most frequently in the lodgepole pine and ponderosa pine and brown rot was more frequent in the Douglas-fir and Sitka spruce. Western hemlock seemed to have both brown and white rots active (Chen H.). The results of this study can't point specifically to either white or brown rot, it can only show the effects of decay caused by rot. For ease of communication however, I will state that a certain rot was shown to be present based on consistency with the effects of the decay. Further study by the Department of Forest Science is underway to determine what exact species of fungus is present.

2. NUCLEAR MAGNETIC RESONANCE (NMR)

2.1 THEORY

The abundance of a molecule like lignin, relative to another, like cellulose, can be determined to some degree of accuracy using Nuclear Magnetic Resonance (NMR). NMR relies on the fact that nuclei can have different energy levels based on their nuclear spin (I), their gyromagnetic ratio (γ), and the applied magnetic field they are placed in (B). When the nuclear magnetic moment is oriented with the applied field, they are in their lowest energy state. Oriented opposing the applied field is the highest energy state. These energy levels are called the Zeeman levels and the Hamiltonian describing the interaction is expressed by the equation:

$$H = -\mu \bullet B = -\hbar\gamma I_Z B_z \qquad (2.1)$$

where μ is the magnetic dipole moment of the nuclei equaling $\hbar\gamma I_Z$. Here $\hbar$ is Planck's constant (h) divided by 2π, and m_I can have $2I+1$ different values between I and $-I$. In the case of carbon, I=1/2 so the only energy levels are $2(1/2)+1=2$, so $m_I = \pm 1/2$. The Zeeman levels are therefore separated by:

$$+\hbar\gamma B_z /2 - -\hbar\gamma B_z/2 = \hbar\gamma B_z \qquad (2.2)$$

When the system is at equilibrium, a slight excess of nuclei will reside in the lowest energy state. At room temperature, the populations of the two energy levels differ by less than 1 part in 10,000 and have a Boltzmann distribution of spins described by the equation $\exp(-E/kT_s)$. E is the energy difference between states and T_s is called the spin temperature, which is described in more detail below. The energy separation between states is on the order of radio frequencies. Therefore an rf pulse can be absorbed by the system and cause a change of state for a distribution of spins.

If a nucleus is pushed into a higher energy state and allowed to relax, it will fall back to the lower energy state at a certain rate determined by its own structure and the molecular structure it resides in. Because there is only one higher energy level, only discrete energy absorption can occur. If you apply energy that is less than is needed to move into the higher energy state then you won't get much energy absorption. If however you apply just the right amount of energy needed, then you will move a greater number of nuclei from the

lower to the higher energy state than from the higher to the lower. This leads to a net absorption of energy from the external source. NMR experiments generally use an oscillating magnetic field to generate these transitions between energy levels. When the frequency ν_o of the oscillating magnetic field is generating the transition "exactly" from low to high, then the frequency is called the resonant frequency. The separation between Zeeman levels will also be equal to $h\nu_o$, which gives the equality (Weissbluth, M, 1978):

$$\hbar\gamma B_z = h\nu_o \tag{2.3}$$

solving for ν_o gives:

$$\nu_o = \gamma B_z / 2\pi \tag{2.4}$$

So all you need to know in order to determine the approximate frequency at which resonance is observed in a sample is the strength of the applied magnetic field and the gyromagnetic ratio of the nuclei you wish to observe. As is discussed later, the precise resonance frequency differs slightly from this value due to local magnetic fields generated within the material.

The torque (τ) the magnetic moment will feel in an applied magnetic field is related to the angular momentum I of the spin and the static field it rests in by:

$$\tau = \gamma \boldsymbol{I} \times B_z \tag{2.5}$$

Torque however also equals the rate of change of angular momentum, which allows a differential equation to be written for the motion of the magnetic moment μ, where $\mu = \gamma \boldsymbol{I}$.

$$d\mu/dt = \mu \times (\gamma B_z) \tag{2.6}$$

The solution to this equation describes the precession of the magnetic moment as it moves around the static field B_z with a frequency ω_L. This is called the Larmor frequency and the solution to the differential equation looks like:

$$\omega_L = -\gamma B_z \tag{2.7}$$

Comparing equation 2.7 to equation 2.3, we see the Larmor frequency is the same frequency needed to be applied in order to stimulate the resonance.

2.2. ROTATING REFERENCE FRAME

In order to view these mechanics from the reference frame of the magnetic moment, we need to transform these equations into the rotating reference frame of the magnetic moment shown in figure 2. This is done quite simply with equation 2.8 that relates any time dependant vector $I(t)$ from the laboratory reference frame S to the moving frame S'.

$$dI/dt = \partial I(t)/\partial t + \omega \times I \tag{2.8}$$

When this is rearranged, it yields an expression for dI/dt, which we know to be equal to torque.

$$\partial I(t)/\partial t = dI/dt + I \times \omega \tag{2.9}$$

Using equation 2.5 and that dI/dt is equal to τ, we see that:

$$\partial I(t)/\partial t = \gamma I \times B_z + I \times \omega \tag{2.10}$$

After a little rearranging gives:

$$\partial I(t)/\partial t = \gamma I \times (B_z + \omega/\gamma) \tag{2.11}$$

Equation 2.11 describes the angular momentum as a function of time in the rotating reference frame. $B_z + \omega/\gamma$ is the field that the magnetic moment oscillates about and is called the effective magnetic field B_e. When $B_z = -\omega/\gamma$, then B_e = zero, which makes $\partial I(t)/\partial t$ = zero, meaning I is a fixed vector in the rotating frame. Here, at this resonance condition, ω is the Larmor frequency ω_L. Having I as a fixed vector in the rotating frame means that, in the laboratory frame, I precesses about B_z.

When an rf pulse is applied to the magnetic moment, it is applied along the x-axis at the Larmor frequency, which sends the nuclei to their higher energy state. This is also referred to as heating up the population to use a thermal analogy. This can be seen with the Boltzmann equation $\exp(-E/kT_s)$, where by giving the population energy you are effectively increasing the spin temperature in the rotating reference frame.

2.3. THE FOURIER TRANSFORM

When the rf field that excited a resonant nucleus such as ^{13}C is turned off, the nuclei that had gained transverse magnetization are then allowed to lose coherence and go back to the

original Boltzmann distribution. This loss of coherence creates a signal that can be measured and is called a free induction decay, or FID, as shown in figure 3. The FID is a time domain signal that can be converted into the frequency domain by a Fourier transform. The frequency domain is generally of more interest because the lines that appear in the frequency domain are resonance lines that are specific to the local environment of the nucleus being observed.

The general procedure for performing a Fourier transform is too take the time domain data $f(t)$ and use equation 2.12 to generate the frequency domain data $f(\omega)$.

$$f(\omega) = \int_{-\infty}^{+\infty} f(t) \exp\{i\omega t\} dt \tag{2.12}$$

The data obtained is not continuous as required by the above equation. Therefore the discrete Fourier transform is used instead.

$$f(\omega) = \sum_{-\infty}^{+\infty} f(t) \exp\{i\omega t\} dt \tag{2.13}$$

In practice the sum can't be carried out from negative infinity to positive infinity. These limits are set by the parameters of the acquisition and any error generated by this is very easily identified. Figure 4 shows a Fourier transform obtained for Hexamethyl Benzene (HMB) while checking the parameters for analyzing the tree samples. The frequencies shown on a frequency domain Fourier transform are directly related to the energy levels that the nuclei were able to absorb.

2.4. NMR ON ^{13}C

NMR is an effective method of studying bulk samples such as these. One highly beneficial aspect of NMR is that it's non-destructive. The actual data collection does no permanent alteration to the sample.

For tree samples such as these, a technique called Cross Polarization Magic Angle Spinning NMR (^{13}C CP-MAS NMR) is used. A diagram of a typical ^{13}C cross polarization pulse sequence is shown in figure 3. Cross Polarization involves adjusting the stimulation power acting on the protons that surround the carbon nuclei, so that the protons and the carbon nuclei require the same pulse width for a 90 degree ($\pi/2$) rotation of the magnetic

moment. When not being stimulated, the magnetic moment is in line with the external applied magnetic field of the superconducting magnet. This is defined as the z axis in the reference frame of the lab. After rotating the protons by a $\pi/2$ pulse directed along the x axis, the precession angle has been changed by 90 degrees and now is in the x-y plane of the rotating reference frame (Monte, F., 2000). The protons are then spin locked, followed by applying rf pulses to both the protons and carbons, allowing the Hartmann-Hahn condition to be met, which is discussed in more detail in the following paragraph. Once the carbons have cooled as much energy as they can, the rf applied to them is shut off, allowing the carbons to relax. During this time a decoupling pulse sequence is applied to the protons, which removes any dipolar coupling between the protons and the carbons. Once the carbons have fully relaxed the entire sequence is repeated.

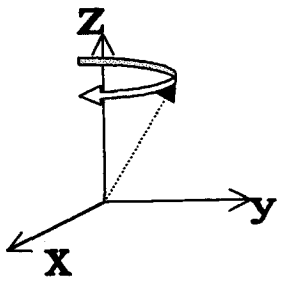

Figure 2. Dotted arrow represents the magnetic moment. Curved arrow shows the path of the end of the magnetic moment as it rotates around the Z axis.

Adjusting the stimulation power so the pulse width conditions are equal is essentially matching the Zeeman splitting of the proton in the effective field and the Zeeman splitting of the carbon in the effective field, in their respective rotating reference frames. This allows for the carbon and the proton to exchange energy via spin-spin interactions (Slichter, C.P., 1996). This is known as the Hartmann-Hahn condition mentioned earlier, named after the people who first realized this as a possible way to strengthen the signal and decrease relaxation time.

This is possible because in order to stimulate a nucleus, one needs to apply a frequency very close to the Larmor frequency. The frequency stimulating the protons is much greater

than the Larmor frequency of the carbon nuclei. The carbon nuclei will therefore be virtually unaffected by the frequency stimulating the protons. The same is true for the ability to stimulate the carbons without disturbing the protons.

Because there is a great abundance of protons per carbon nuclei, the protons surrounding the carbon nuclei act as an energy reservoir and will help dissipate the energy of the carbon nuclei, bringing them back into equilibrium with the external field more quickly (Monte, F., 2000). This shortened relaxation time allows for a shortened acquisition time. This allows for many more acquisitions in the same period of time. The greater number of acquisitions leads to a greater signal average and therefore a cleaner spectrum.

The term spin-lock is the process of keeping (locking) the protons so that, in the rotating frame, they are oriented or magnetized in the same direction as the rf field. This is done by changing the phase of the rf pulse shortly after an initial $\pi/2$ pulse that flips the magnetic moment along the y-axis. Once the phase is changed to match the phase of the magnetization, the protons are then 'locked' by irradiating them with this new phase. In the rotating frame of reference, the protons are now oriented along the rf field and therefore in a lower energy state. Using the spin temperature analogy they could be said to have a lower spin temperature in the rotating frame. Keeping the protons in a lower energy or cooler state during the thermal contact between the protons and the carbon nuclei helps facilitate the relaxation of the carbon.

Cross polarization also strengthens the signal by increasing the magnetization of the carbon nuclei. To use a thermal analogy is helpful to understand the process and can be done by relating energy to temperature. Consider the carbon nuclei as being heated when they are given energy and the protons acting as a thermal reservoir as there are so many more protons relative to carbons. The protons are prepared in a cooler spin state as described above. As the carbon exchange energy with the proton reservoir, the carbons will cool down. As the temperature of the carbons drop, the magnetization of the carbon will increase, resulting in a stronger signal.

In order to help identify the peaks on the spectrum I used a dipolar dephasing pulse sequence. This is generated by inserting a delay period, usually between 40μs-100μs, without ^{1}H decoupling between the cross-polarization and acquisition portion of the CP-MAS pulse sequence.

As stated earlier, there are many peaks on the Fourier transform (FT) spectrum. This is due to the fact that there are many different local environments for the carbon nuclei in the sample. Some decay very rapidly, especially if they are surrounded by a larger number of protons and able to give up their energy easier. Other carbons have fewer protons near and therefore take longer to relax. By inserting a delay before acquisition, you separate out the carbons that decay rapidly and only acquire the decay of the carbons that took a longer time. The FT spectrum will therefore not have that peak(s) that relate to rapidly decaying carbon. The rapidity of the decay is further enhanced by not having decoupling during this delay period, allowing for dipolar and spin-spin decay processes to take place between the protons and carbon nuclei.

The signal on the slowly decaying carbons is a weaker signal, because even though they take longer to decay, you are still ignoring a good portion of their decay process. In order to get a good spectrum using dipolar dephasing I generally had to double the number of acquisitions. This is time consuming, so I only used the technique a few times until I was reasonably sure I had correctly identified the peaks relating to the rapidly decaying carbons.

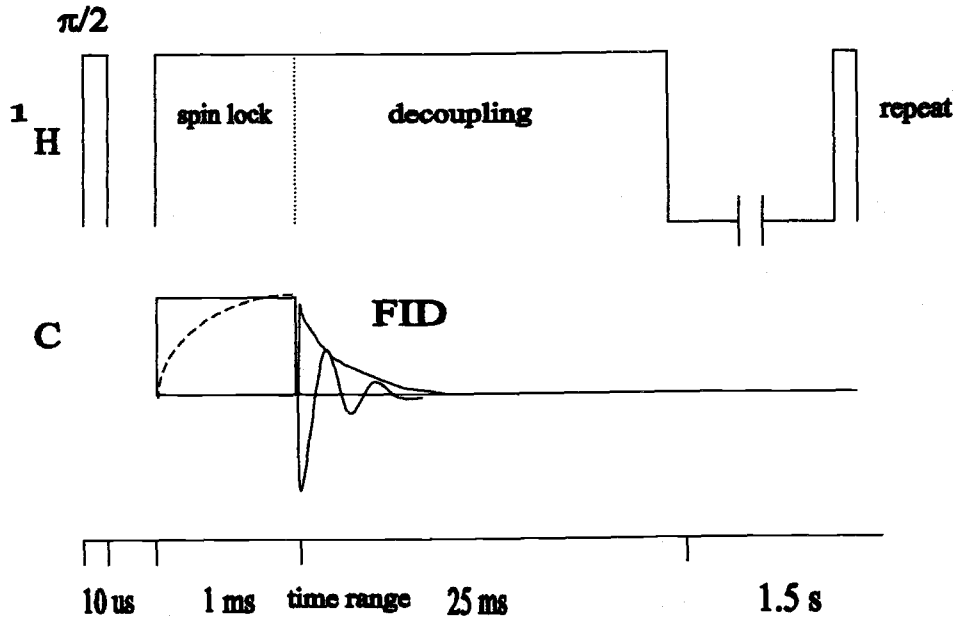

Figure 3. Diagram of the pulse sequence on top and the resulting action of the magnetic moment of the proton and the carbon nuclei and the timeline of the events.

2.5. MAGIC ANGLE SPINNING AND TOSS

Magic Angle Spinning (MAS) is used through this whole process. This involves tilting the sample container so that it makes an angle ξ with the applied field and spinning the sample rapidly about this angle. This is called the magic angle for at this angle, many of the line broadening effects go to zero (Slichter, C.P., 1996). This can be seen in equation form by writing the broadening effects in the same form and seeing that nearly all contain the element $(3 \cos^2 \xi - 1)$ which goes to zero when ξ equals 54.7 degrees, the magic angle. It is spun at this angle in order to rapidly rotate all the molecules, which averages their orientations as if they were in a liquid sample. Because of the three dimensional nature of the electronic shielding, the chemical shift for solids is anisotropic due to the dependence on the orientation of the nuclei to the applied static magnetic field. Spinning the sample effectively removes this dependence and narrows the anisotropic line-broadening effects.

It would also have been to my benefit had I run all my acquisitions using a TOSS pulse sequence, which is a Total Suppression of Spinning Sidebands. Sidebands are generated when a sample is spun and can be identified by their location relative to the peak that they are being generated from. They appear at intervals of the spinning frequency on a frequency spectrum as demonstrated using hexamethylbenzene in figure 4. I tried a TOSS sequence on a few samples, but came to the conclusion that it caused too much distortion in the spectrum to obtain usable data. This was quite unfortunate, for sidebands can be large at high NMR fields. On the other hand, the TOSS sequence seemed to be a weaker signal, so I would have had to spend a great deal more time per sample taking more acquisitions. By spinning at 5kHz I hoped this would push the sidebands out farther and minimize the effect they would have. For the parameters I used, spinning at 5kHz would move sidebands out approximately 58.6 ppm on both sides of the peak it is generated from. I accepted this also because we weren't concerned with the actual amount of lignin and cellulose, but rather the relative change over time, which I believe could be determined adequately within these limitations.

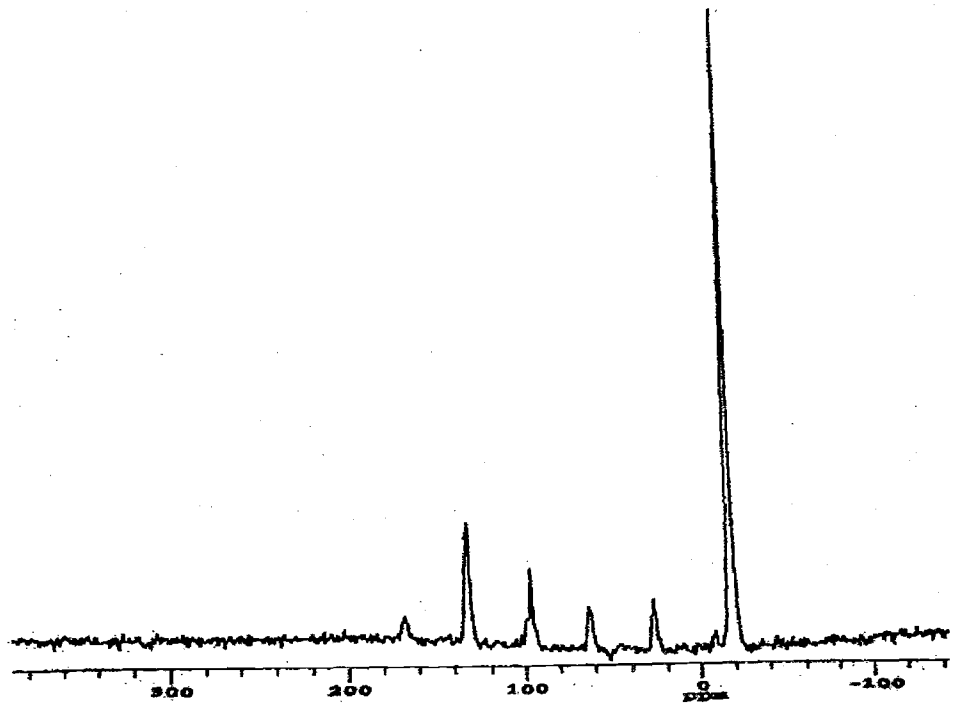

Figure 4. CP-MAS NMR Spectrum of HMB

2.6. EXPERIMENTAL PROCEDURES

2.6.1 Parameters

Before I started processing my samples, I needed to establish parameters that would maximize my signal. It is a standard practice to use hexamethylbenzene (HMB) when adjusting parameters for studying carbon nuclei, so that is what I used. At this point it was also a good time to make sure I was able to improve the signal using cross polarization. Once a cross polarization free induction decay (Fid) with adequate signal to noise ratio (≈40/1 in fig.4 depending on method of measuring) was achieved, I was ready to establish a benchmark from which to measure the chemical shifts.

In order to establish a benchmark to measure all the chemical shifts (see 2.6.2) of the different carbon nuclei, I used a widely used chemical standard called tetramethylsilane [TMS,$(CH_3)_4Si$]. TMS is widely used because it has a Larmor frequency that is much lower than most molecules with carbon in them. Therefore the signal sits on one side of the carbon spectrum and can be used as a common reference for all the carbon signals.

I obtained a bottle of liquid TMS and loaded a small tube called a pencil rotor with it, which is described in more detail in section 3.3. Being a liquid, it had a long relaxation time, so I had the recycle delay set at 5 s and ran 100 cycles in order to obtain an adequate spectrum. Recycle delay is the delay between trials or cycles, which is needed for the system to come back into equilibrium with the external field. The Fourier transform produced a line at –31.5 ppm so for the data collection on the tree samples, I set the zero point to –31.5 ppm and measured all the carbon peaks from this zero.

I needed to maximize the resolution I would obtain in the spectrum so I needed to choose appropriate parameters to use when acquiring my data. I expected the carbon spectrum to fall within 0 ppm to 220 ppm so I wanted to make sure I had a spectrum that at least included these end points. By choosing a sampling interval of 25μs, I could expect that my spectrum width would roughly be between 235 ppm and –235ppm. This is shown with formulas 2.14 and 2.15. The term dwell time refers to the sampling interval.

$$\text{Spectrum Width} = 1/(\text{Dwell time}) \qquad (2.14)$$

$$\text{Ppm Width} = [\text{Spectrum Width} \div \text{Spectrometer Frequency}] \times 10\text{^}6$$

$$\text{Ppm Width} = [1/(25\mu s) \div [85.367\ \text{MHz}]] \times 10\text{^}6 = 468\ \text{ppm} \qquad (2.15)$$

My pulse width was determined by matching the power settings on the proton channel and the carbon channel so that they required the same pulse width for a 90 degree rotation. I first determined the pulse width for the proton channel at maximum power and then adjusted the carbon channel's power until it had the same pulse width condition. My pulse width ended up being 4.65 us.

2.6.2 Chemical Shifts:

The Fourier transform of the ^{13}C signal using these parameters is a spectrum that looks like Figure 5. The integrated area under one of the peaks of the spectrum represents the abundance of a carbon nucleus in a certain molecule that absorbed energy at a certain frequency. There are many different peaks because there are many different chemical environments for the carbons. When these compounds are placed in a strong external field,

the orbiting electrons will be strongly affected and the currents produced will generate a local B field in opposition to the applied field (Weissbluth, M., 1978). This local B field will be unique to each nucleus in the molecule as long as the local structure surrounding the nuclei is different. The effect of the local B field shields the nuclei from the applied field so that the observed resonant frequency is slightly less. This shift in resonant frequency is called the chemical shift. Therefore each class of nuclei will have a unique chemical shift, yielding a different peak in the Fourier transformed spectra.

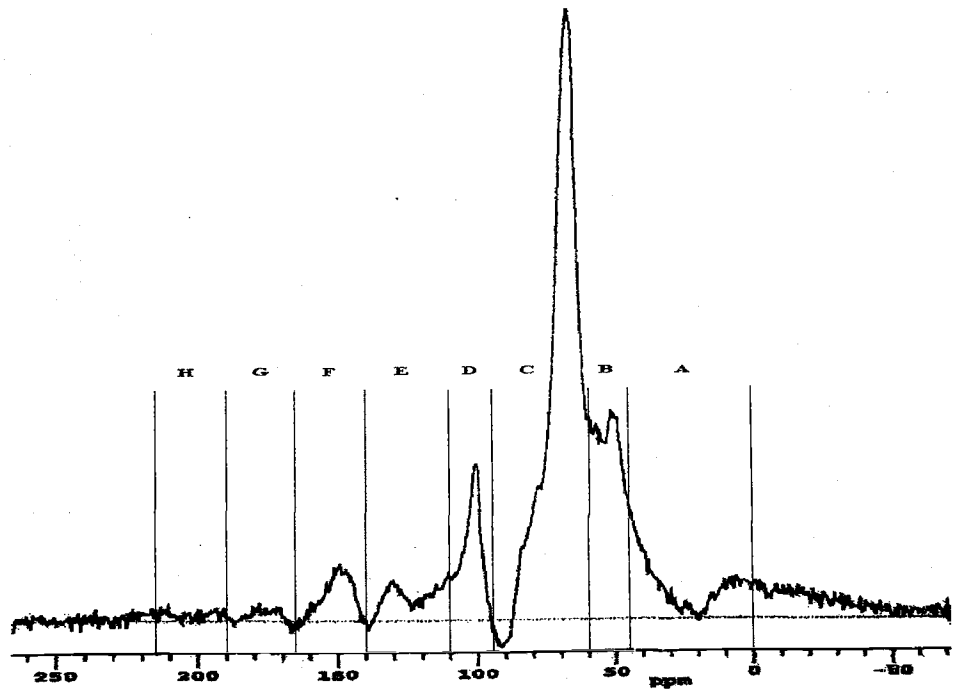

Figure 5. ^{13}C-CP-MAS NMR Spectrum of a typical wood sample. Lines show the divisions of chemical shifts used in my analysis.

The chemical shift regions were determined from observation of minima in the spectrum and also from a literature review of many different studies conducted to identify these regions. I settled on using the chemical shift regions outlined in (Preston, C.M., 1998). These regions are shown in Figure 5 and were identified as follows: (A) aliphatic, 0-47 ppm; (B) methoxyl, 47-60 ppm; (C) O-alkyl, 95-110 ppm; (E) aromatic, 110-140 ppm; (F) phenolic, 140-165 ppm; (G) carboxyl, 165-190 ppm; (H) carbonyl, 190-215 ppm. Using a technique called deconvolution, one can pick out the peaks within the spectrum and model them with gaussian or lorenzian peaks. This is useful because within the spectrum the peaks are often overlapping. Dividing up the chemical shift regions just with vertical lines is an approximation, so by using deconvolution the results can possibly be more precise. The drawback to deconvolution is that it can be time consuming and it in itself is an approximation in that we really don't know if the peak is gaussian, lorenzian, or some combination. In the interest of time, as I had a lot of samples to process, and due to the

qualitative nature of my goal, I chose to use the approximation of just taking the divisions mentioned above, and not using deconvolution. Most studies of this nature that I reviewed don't bother with deconvolution, as they are also focused on more qualitative results where the small amount of error introduced is inconsequential. By comparing the integrated areas I was able to determine the change in lignin and cellulose over time.

Before I was able to compare the integrated areas, I had to multiply the areas with a correction factor that corrected for the contact time I chose. I had a contact time of 1ms, which is standard for samples like these. However, the contact time is the time allowed for the protons and carbons to exchange energy. A shorter contact time would (Preston, C.M. et al., Canadian Journal of Botany, 1997) over emphasize the molecules with shorter decay rates and under emphasize the longer decaying molecules. A longer contact time would do just the opposite. I, therefore, had to adjust for this by using a scaling factor that scaled the integrated areas in the Fourier transform accordingly for a 1ms contact time (Preston, C.M., 1997).

Lignin and cellulose peaks occur at a couple of different points along the spectrum. This makes sense because the carbon in the lignin and cellulose molecules are surrounded by different combinations of protons and oxygens as shown in Figure 6a and 6b. This makes for different relaxation rates. A widely accepted formula used to determine the amount of lignin and cellulose in an NMR spectrum is (Preston, C.M., 1998)

$$\text{Lignin carbon} = 4.5F + B \tag{2.15}$$

And to find the amount of cellulose,

$$\text{Polysaccharide carbon (cellulose)} = 1.2(C - 1.5F) \tag{2.16}$$

The letters B, C and F refer to the regions described above and diagramed in Figure 5.

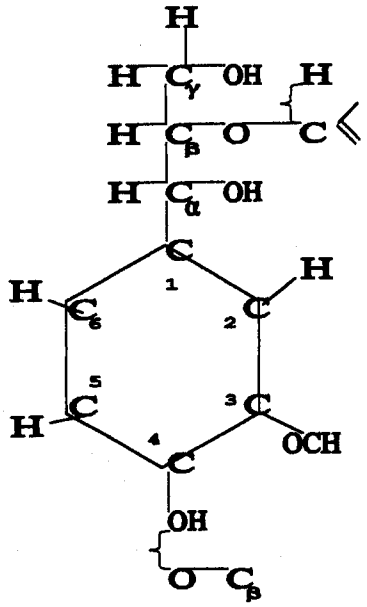

Figure 6.a. Lignin molecule

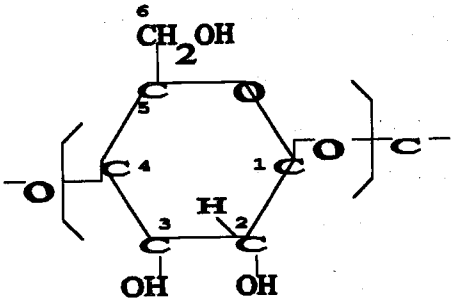

Figure 6.b. Cellulose molecule

3. DATA COLLECTION—BASIC SETUP AND EQUIPMENT

3.1. MAGNET

All the data were collected using a superconducting magnet made by American Magnetics, Inc. The magnet was kept at its maximum designed limit of 8 Tesla as other people in our group were conducting experiments that benefited from this. The magnet has a 3 inch diameter bore in which to place our probes. The theoretical homogeneity of the field is 1 ppm over a 1 cm diameter sphere, though I tested using distilled water and found it to be closer to 1.5 ppm.

3.2. SPECTROMETER

The spectrometer used was the CMX360-1436 Chemagnetics operating at 85.367 MHz. The spectrometer has two channels, one of which is dedicated for proton NMR. This setup allows for double resonance experiments. Both channels use radio frequencies generated by PTS 500 synthesizers that have a frequency range of 1 MHz to 500 MHz. The carbon channel is then amplified by linear rf pulse amplifier from American Microwave Technology, Inc., and an ENI 5100-NMR amplifier is used for the proton channel. From these amplifiers the rf pulses are applied to the probe.

3.3. PROBE

The double resonance probe I used is also made by Chemagnetics. It's a special double resonance probe in that it can also be used for magic angle spinning (MAS). The sample containers were 5 mm outside diameter spinners, also called pencil rotors, with a zircona casing and Kel-F spinner tip, end cap and spacers. Kel-F doesn't produce a signal in ^{13}C CP-MAS NMR experiments (CMX Users Guide, Chemagnetics Inc.), but I did do a run

using an empty spinner to see if I obtained a signal. Luckily I did not. Had I obtained a signal, I would have had to subtract the empty rotor signal from all of the sample signals.

3.4. DATA COLLECTION

The data were collected using Spinsight and processed mostly with Spinsight. Spinsight is a very specific software package used for the processing of NMR data. The MAS frequency was 5000 Hz, with a recycle time of 1.5 seconds. This gave a total time for one acquisition to be 1.526 seconds. I generally took about 10,000 acquisitions per sample, which equaled about 4 hours total acquisition time per sample. The contact time was 1 ms. Contact time is the amount of time that both the protons and the carbon nuclei are in contact, or the amount of time that the protons are helping the carbon to relax.

3.5. SAMPLE PREP

In order for the samples to be studied using CP-MAS NMR they have to be dried and ground using a Wiley mill to a powder of, at most, a 0.1 mm diameter. This enables the sample to be packed into the spinner tightly. If the packing wasn't tight, the sample could shift around in the spinner as it is spun. This is bad because this could cause the spinner to wobble, causing damage to the probe. This would also give bad data, for the different portions of the powdered sample wouldn't all be spinning at the same rate

4. RESULTS

4.1. RAW DATA

The data obtained do, to a reasonable degree, back up the conclusions that the other analyses have yielded. The bar graphs shown in figure 7 show the percent of lignin and cellulose, relative to the whole sample, for each time period studied. The graphs are grouped by species of tree studied.

As you can see in the graphs, the western hemlock (THSE) showed a dramatic decrease in cellulose over time corresponding with an increase in lignin in both the sap and bark samples. This is rather clear evidence that at least brown rot must have been present in order to produce such a large decrease in the cellulose structure.

The Douglas fir (PSME) species only showed a definitive change in the sap sample where the cellulose decreased from 57% to 34% over 36 years, corresponding to a virtually symmetric increase in lignin, 36% to 57%. The bark and resin samples show much less change and weren't very conclusive aside from showing a decrease in lignin in the bark sample from 56% to 43%.

For the sap sample from the Sitka spruce (PISI) species, I observed the cellulose decrease from 54% to 34% over 33 years while the lignin increased from 42% to 60%. The bark and resin both show a little decrease in lignin and the bark shows a small decrease in cellulose as well.

The lodgepole pine (PICO) sap sample showed a small decrease in cellulose from 53% to 49% over 22 years with very little change in lignin. The bark sample, on the other hand, showed a small increase in cellulose; from 40% to 45% over 22 years, and a decrease in lignin, 48% to 44%. This is within my error estimate of +-5%, so it may mean nothing. However this could be due to white rot attacking the lignin and cellulose, but at slightly different rates, resulting in an increase in the percentage of cellulose.

The ponderosa pine (PIPO) sap sample shows a decrease in cellulose starting at 57% at 1 year to 40% at 22 years corresponding with a small increase in lignin of 35% at 1 year to 39% at 22 years. The bark sample also shows a decrease in cellulose going from roughly 41% at 1 year to 34% at 22 years corresponding with small increase in lignin, from 42% at 1 year to 49% at 22 years.

Figure 7.1 through 7.5 shows the percentage of lignin and cellulose over time.

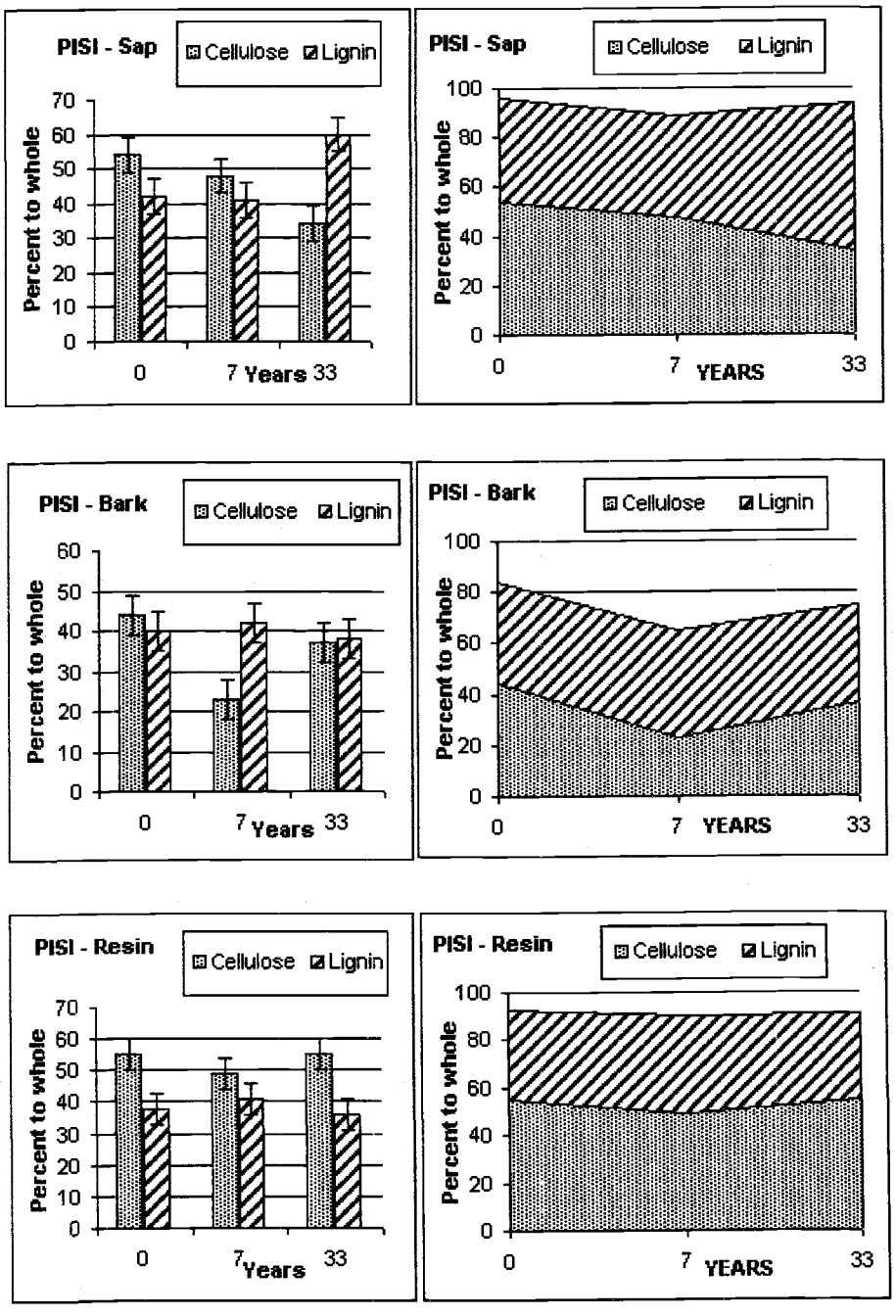

Figure 7.1 Sitka spruce

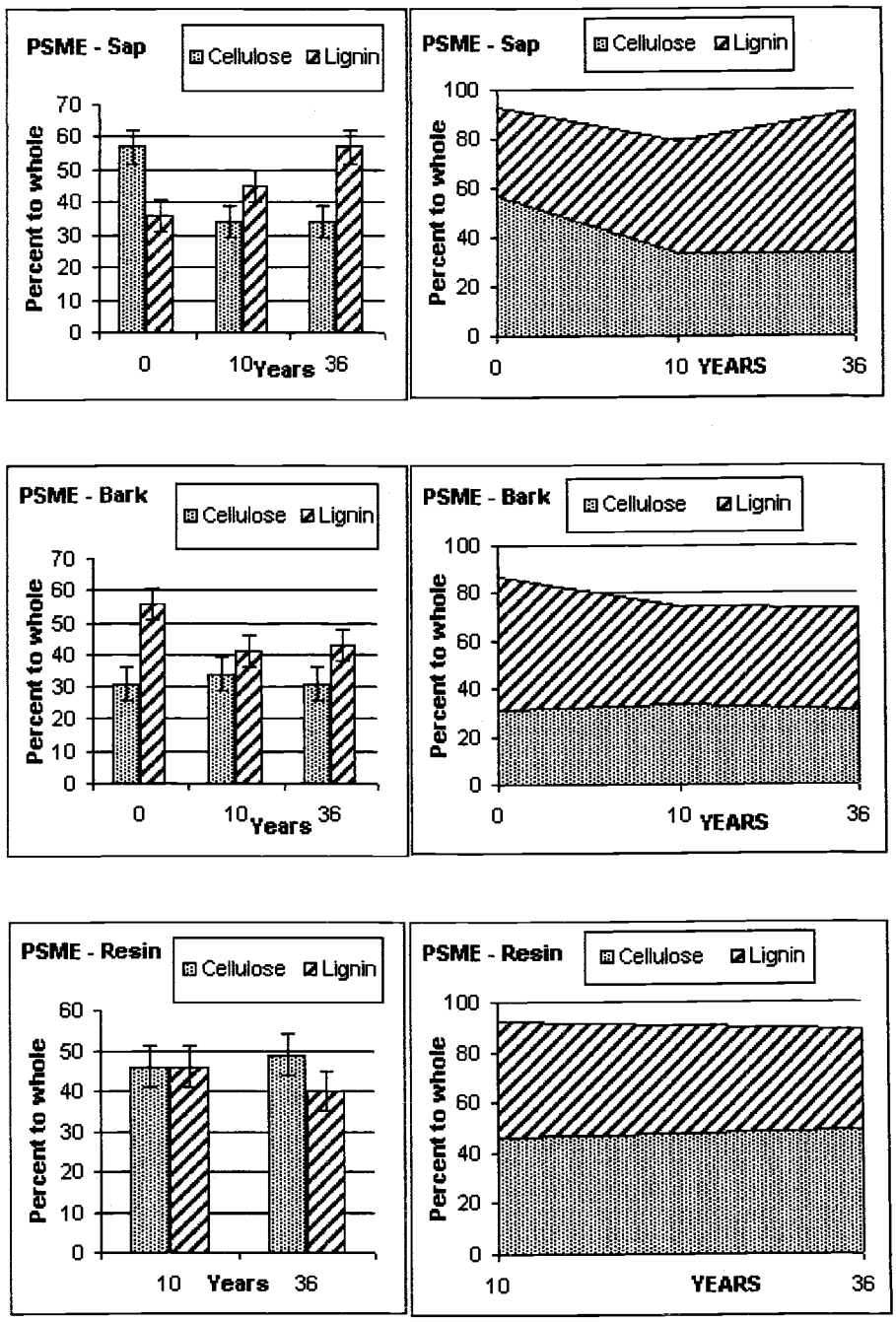

Figure 7.2 Douglas fir

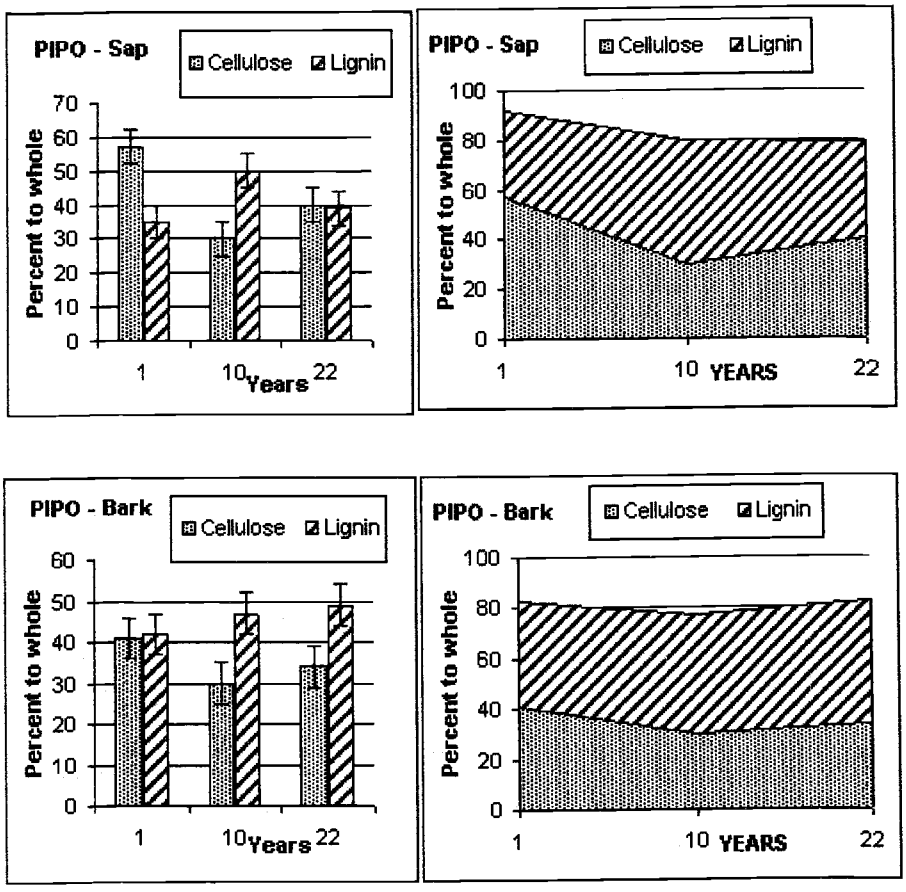

Figure 7.3 ponderosa pine

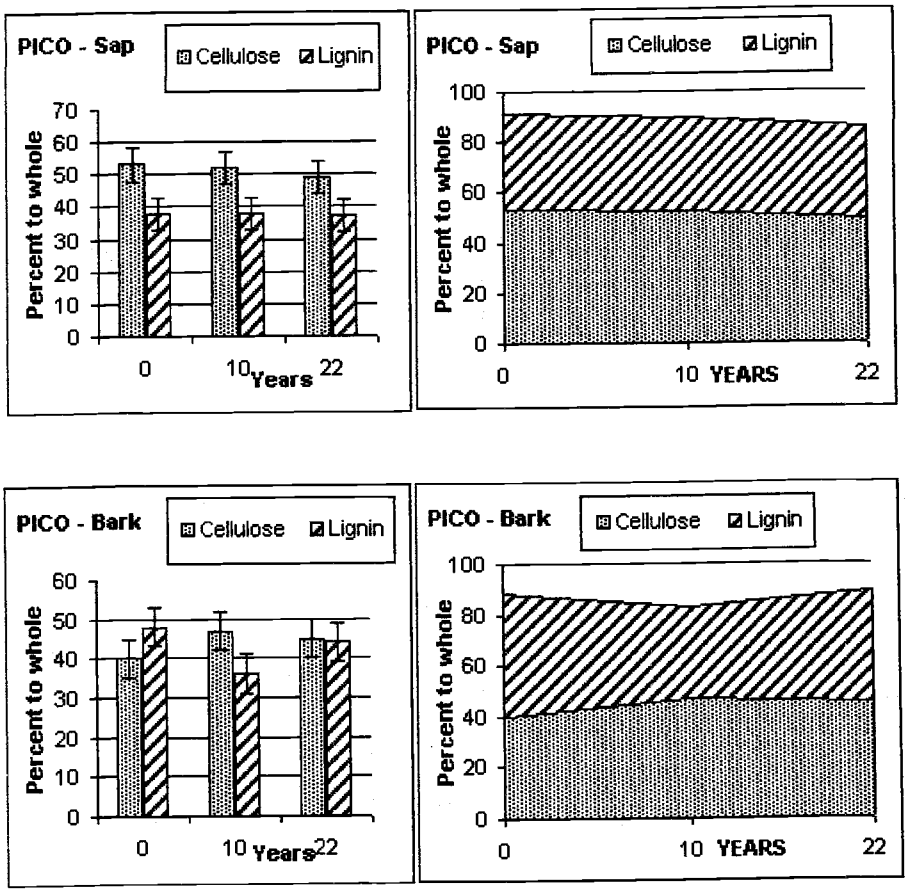

Figure 7.4 lodgepole pine

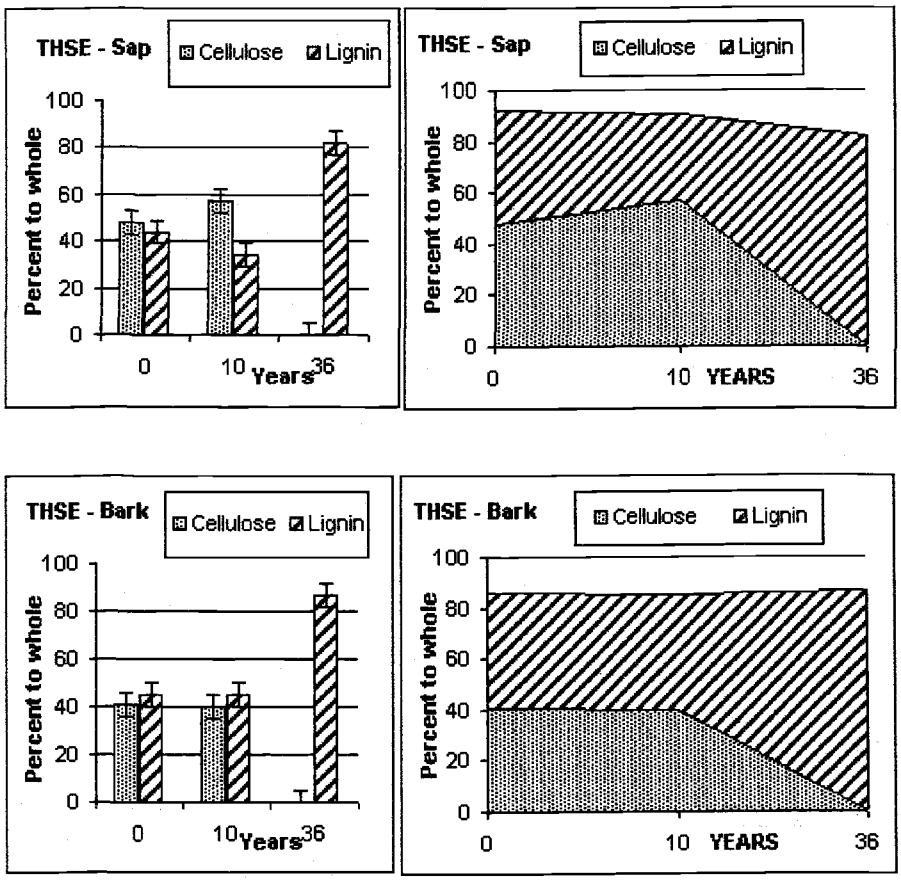

Figure 7.5 western hemlock

4.2. ANALYSIS AND COMPARISON TO OTHER ANALYSIS

As you look at the bar graphs you may notice that the decrease and/or increase in cellulose and lignin isn't uniform. For example, looking at the THSE sap sample you can see that for the first 10 years the percent of lignin decreases and the percent of cellulose increases. Because we think that lignin can only be consumed by white rot, we know that white rot is present and seems to be mostly attacking the lignin here. For the following 26 years however we see that the cellulose gets totally wiped out, leaving mostly lignin. This could be caused by brown or white rot or a combination of both white and brown rot.

If we turn our attention to the THSE bark sample we see something a little different. We see no change at all relative to one another in the first 10 years, therefore no brown rot yet. In the next 26 years we see the cellulose get totally wiped out, and what looks to be a large amount of lignin left. This is clearly a product of brown rot being present, though we can't tell if white rot was present as well without looking at the total mass change.

The PIPO sap sample on the other hand shows us something interesting. During the first time period (1 to 10 years) we see a definitive drop in cellulose pointing to at least brown rot being present. The next 12 years though show the lignin being consumed as well indicating that there must also be some amount of white rot present at this point. The bark on the other hand shows a more pure brown rot picture, with only a hint that white rot may be present in later years.

The PISI sap sample shows definite brown rot attacking the cellulose, leaving the lignin unaffected. The bark also showed brown rot, especially in the first 7 years. The second time period would seem to indicate white rot being present also, for the lignin must have decreased relative to the cellulose for the percentiles to be as equal as they are. The resin sample doesn't definitively show any rot taking place relative to one another, so we know that at least brown rot wasn't present.

The PSME sap sample shows a very clear case of brown rot noting the decline in cellulose with the corresponding increase in the percent of lignin. Based on that it would seem that at in this part of the tree, white rot is not present. The bark on the other hand isn't as conclusive. Here we see a decline in lignin with the percent of cellulose remaining mostly constant. This points to at least white rot being present. The resin sample shows no conclusive change in ratio but leaned on the side of possible white rot. One way of

checking this would be to use find out the total mass loss in the sample. Because my analysis shows that the ratios stay the same at least indicates that probably brown rot isn't present, but if we knew whether or not they both lost mass then we would know that white rot was to blame.

The PICO samples of sap and bark did not definitively show evidence of decay relative to one another over the 22 years studied. This at least tells us that there probably was very little or no brown rot present. There could be white rot but as I indicated earlier, we would need to look at the total mass lost to see if they were losing mass at an equal rate. To be so consistent in the sap sample suggests that very little, if any, white rot is present.

According to previous research from the Department of Forest Science at OSU (Chen, H., 2001) conducted on these samples, it was found that ponderosa pine and lodgepole pine both contained a high amount of white rot; between 79 and 84%. Brown rot was found mostly in the wood of Douglas fir (56%) and Sitka spruce (72%) and western hemlock contained both white and brown rot. These statistics do seem to agree quite closely with the analysis of my data as shown in the grid in table 2. My research couldn't determine the percentage of rot in the sample but could show the presence of the rot.

Results of Present Study vs Previous Forestry Results

	Sap Wood (other study)	Sap Wood (present study)	Bark (present)
THSE	Even Amounts of Both	White and probably Brown	Brown Rot, possible White
PSME	More Brown than White	Brown Rot	Brown and White Rot
PISI	Brown Rot, very little White	Brown Rot	Brown Rot, some White
PICO	Little Brown, Mostly White	No Brown	No Brown
PIPO	Little Brown, mostly White	Brown Rot, later White Rot	Brown Rot, possible White

Table 2. Table comparing present results with previous results.

4.3. ERROR ANALYSIS

In order to get a feeling for what kind of error existed in my experiment, I looked over all the different parameters that could impact the initial analysis of the raw data. The first and most obvious place for error to occur would be the initial benchmark from which the resonance shifts were measured. I'm referring to the TMS sample I used to place the zero point. First possible error would be that I didn't place it well, so I re-measured the point and estimated how far off a person could reasonably be and not know it. Another benefit to remeasuring is that as time passes, the strength of the magnet slowly declines, shifting the placement. By remeasuring I could see if there was any drift from when I measured it the first time. After determining the amount I may have been off (<1ppm give or take) I then reanalyzed a sample with the new zero point to see how much it could change my results.

I also ran a number of samples more than once to see if my results would reproduce themselves, and what kind of difference, if any, would exist between the two. In general the samples reproduced the previous trials results very well with the lignin and cellulose amounts deviating by three to five percent. Some trials obviously didn't go well and were redone. I believe this was mostly because I either packed the sample holder incorrectly and the spinning was therefore corrupted, or there was a technological error with an amplifier during these trials. These corrupted trials were easily identified.

I had enough sample from each part of the tree that I was also able to pack more than one rotor from each sample container. This allowed for further error checking in order to see if the spectrum was truly reproducible within a reasonable error margin. This was only done for a few samples as it is time consuming.

In order to try to gauge the effects of the spinning sidebands, I increased the spinning of the rotors from 5 k to 6 k, which moved the sidebands out 11.7ppm farther from the generating peaks and also made the sidebands smaller. To locate a sideband in ppm, divide the spinning rate, in this case 5000 and 6000 Hz, by the spectrometer frequency of 85.367.

Originally the sidebands were located at ±58.57 ppm of the generating peaks. Increasing the spinning rate to 6000 Hz moved the sidebands out to ±70.28 ppm from either side of their generating peaks. I then processed the sample as I had done previously and compared the two results. There was a small difference between the two trials, but was still within four percent of the original. Interestingly, the shift for both the lignin and cellulose was an increase in both by roughly the same amount, so their amounts relative to one another were closer to about 1 or 2 percent shift.

Overall the amount of error that existed in my experiment resulted in a possible shift of ± 5 percent in the amount of lignin or cellulose relative to the whole. This can be seen in the error bars on the bar graphs in figure 7.

5. SUMMARY

5.1. SUGGESTIONS FOR FURTHER STUDY

Ideally, for this kind of study, it would be nice to have had more time periods for each kind of sample. Three data points over a 30 year period is better than two data points but I believe four would be ideal. Three was not enough because it did not provide enough detail of the degrading action. Having more time periods also provides the benefit of having a more continuous view of the action, which helps for error checking during the experiment. For example, with three points it may not be apparent if a sample should be run again, but with four points it would be more apparent. Five points would be too many given the amount of time needed to acquire the data.

It would also be useful to try running a TOSS sequence again. At the beginning of my project I was not as familiar with phasing and how the spectra would look, so I could have spent more time trying to make a TOSS sequence work. The alternative to trying to make the TOSS sequence work would be to ramp down the magnet to 2 or 3 Tesla. This would make the spinning sidebands quite a bit smaller and minimize the need of a TOSS sequence. Taking the magnet to a lower field does have some disadvantages such as a lower sensitivity resulting in a worse signal to noise ratio. This would result in needing quite a few more acquisitions to achieve reasonable data. This would only be worth doing for one or two trials in order to compare spectra for sideband distortion.

5.2. CONCLUSIONS

The use of ^{13}C CP-MAS NMR is helpful in determining the ratio of lignin to cellulose in tree samples. The information gathered here using this technique showed when brown rot existed and when it did not exist, and less directly when white rot must have been present. Used in conjunction with other studies such as wet chemical analysis and mass measurements, ^{13}C CP-MAS NMR can offer useful data in a non-destructive, reproducible way, and confirm or extend conclusions reached through these other means.

It was very hard to know when white rot was present with this study as it can attack both lignin and cellulose. The only way to be sure of the presence of white rot was to observe the percentage of lignin decreasing. For all these results studies other than NMR would need to be done to see if white rot was present in the time periods not mentioned. My results do show the percentage of lignin decreasing four separate times, which indicates that white rot must be present. The Douglas fir bark sample showed definite white rot during the first 10 years. The ponderosa pine sap showed white rot in the 10 to 22 year period. Sitka Spruce showed some white rot in the bark from 7 to 33 years, and the western hemlock showed some white rot in the sap in the first 10 years.

The effects of brown rot were much easier to see in this study. Virtually all the sap and bark samples showed the effects of brown rot at some point. The Douglas fir was the only species, other than lodgepole pine, not to show any effects of brown rot in the bark of the tree, only white rot. The Douglas fir did show brown rot decay in the sap for the first ten years. Ponderosa pine showed evidence of brown rot decay in the first 10 years in the sap and the bark. The Sitka spruce species analysis showed brown rot decay in the bark for the first 7 years and in the sap for the entire time studied of 33 years. The lodgepole pine was the only species to not show any brown rot decay in the sap or bark for the entire 22 year period studied. The western hemlock also made itself distinct by not showing any definitive brown rot decay for the first 10 years, but showed massive brown rot decay in both sap and bark during the following 26 years studied.

There are direct applications for the above findings. For example, if a forester was planning on logging an area of forest containing western hemlock that is in a climate similar to the climate from which my samples were taken, the forester could be reasonably assured that there would be soil stability for the first 10 years as there was only a little decay from white rot during that time period. However the following years showed massive decay from brown rot, so to ensure soil integrity, new trees should be planted and giving time to grow before the decay advances too far. If the forester was in a forest of Douglas fir, then quicker action must be taken as there was evidence of both white and brown rot in the first 10 years. This would be true for the ponderosa pine and Sitka spruce as well, as there was brown rot evidence in the first time period and white rot in the following years.

BIBLIOGRAPHY

Chen, H., Harmon, M.E., Griffiths, R.P., Decomposition and nitrogen release from decomposing woody roots in coniferous forests of the Pacific Northwest: a chronosequence approach, (*Canadian Journal of Forest Research* 31, 246 2001)

CMX Users Guide, *Double Resonance MAS Probe*, Chemagnetics Inc.

Monte, F., *NMR Study of 1,4-phenilene-bis(dithiadiazolyl), Soil Organic Matter and Copper Aluminum Oxide*, Ph.D. Thesis, (Oregon State University, 2000)

Preston, C.M., Trofymow, J.A., Sayer, Brian G., Niu, Junning *Canadian Journal of Botany*, 75, 1601 (1997)

Preston, C.M., Trofymow, J.A., Niu J., Fyfe, C.A., 13CPMAS-NMR spectroscopy and chemical analysis of coarse woody debris in coastal forests of Vancouver Island, *Forest Ecology and Management* 111, 51 (1998)

Slichter, C.P., *Principles of Magnetic Resonance,* (Springer, New York, 1996)

Weissbluth, Mitchel, *Atoms and Molecules*, (New York : Academic Press, 1978)